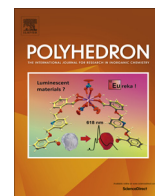




Contents lists available at ScienceDirect

Polyhedron

journal homepage: [www.elsevier.com/locate/poly](http://www.elsevier.com/locate/poly)

# Metal-dependent ribbon and self-penetrated topologies in nitroaromatic-sensing zinc and cadmium coordination polymers with terephthalate and dipyridylamide ligands

Megan J. Wudkewych, Robert L. LaDuca\*

Lyman Briggs College and Department of Chemistry, Michigan State University, East Lansing, MI 48825, USA

## ARTICLE INFO

## Article history:

Received 20 July 2015

Accepted 8 October 2015

Available online xxxx

## Keywords:

Cadmium

Zinc

Coordination polymer

Crystal structure

Nitroaromatic detection

## ABSTRACT

Hydrothermal reaction of the requisite metal nitrate, potassium terephthalate ( $K_2\text{tere}$ ) and the dipyridylamide 3-pyridylisonicotinamide (3-pina) afforded a pair of crystalline coordination polymers whose dimensionality and topology depends critically on the metal coordination environment. The two new crystalline phases were structurally characterized via single-crystal X-ray diffraction.  $\{[\text{Zn}(\text{tere})(3\text{-pina})_2]\cdot 2\text{H}_2\text{O}\}_n$  (**1**) manifests a 1-D zig-zag ribbon motif with monodentate 3-pina ligands.  $[\text{Cd}(\text{tere})(3\text{-pina})_2]_n$  (**2**) displays a self-penetrated 3-D network with  $4^46^{10}8$  **mab** topology. Thermal and luminescent properties of these two new materials are also presented. Both **1** and **2** show capability as sensors for nitroaromatic compounds via luminescence quenching, with better absorption for nitrobenzene than the more sterically bulky analyte *m*-nitrophenol.

© 2015 Elsevier Ltd. All rights reserved.

## 1. Introduction

Over the past fifteen years, there has been an intense research spotlight on the exploratory synthesis and structure of crystalline coordination polymer solids. Interest remains strong due to potential of this genre of solid state materials in gas storage [1], molecular separations [2], ion exchange [3], heterogeneous catalysis [4], and as luminescent explosives trace detectors [5]. The undeniable esthetic appeal of their underlying 1-D, 2-D, or 3-D topologies also provides an impetus for continued research efforts [6]. Divalent zinc or cadmium ions have proven efficacious choices as the requisite cationic component, predicated on their closed shell  $d^{10}$  electronic configurations. Full *d* shell population results in forbidden visible light *d-d* transitions, imparting the transparent visible light spectral window required for fluorescent sensing [7] or second harmonic generation applications [8]. Due to the lack of crystal field stabilization for divalent zinc and cadmium ions, coordination polymer structure direction is ascribed to the combined effects of ligand donor disposition, carboxylate binding mode and steric requirements, as opposed to a specific preferred metal coordination geometry.

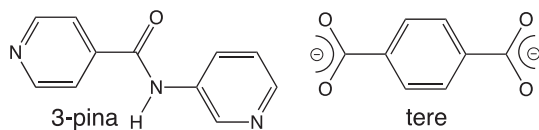
A myriad number of different topologies have been reported for divalent zinc and cadmium coordination polymers with aromatic dicarboxylate and neutral dipyridyl linkers [9–14]. Some of these

display intriguing and rare self-penetrated networks, in which the shortest rings within the topology pass through other shortest rings. For example,  $[\text{Cd}(\text{Hph})_2(\text{bpy})]_n$  (pht = phthalate, bpy = 4,4'-bipyridine) manifests a self-penetrated 6-connected 3-D network with  $5^{10}6^{47}$  topology [9]. Using the kinked and hydrogen bonding capable dipyridyl ligand 4,4'-dipyridylamine (dpa) afforded  $[\text{Cd}(\text{pht})(\text{dpa})(\text{H}_2\text{O})\cdot 4\text{H}_2\text{O}]_n$ , which displays a unique chiral self-penetrated 4-connected  $7^48^2$  **yyz** topology based on interlocked helical subunits [10]. In other cases, this combination of ligand types has allowed self-assembly of coordination polymers with enticing adsorptive properties. For example, the desolvated apohost of  $\{[\text{Zn}_2(\text{tere})_2(\text{bpy})]\cdot \text{H}_2\text{O}\cdot \text{DMF}\}_n$  can separate challenging mixtures of low molecular weight alkanes [11].

In comparison to coordination polymers containing bpy or dpa ligands, there are fewer reports of related materials containing the hydrogen-bonding capable dipyridylamide ligand 3-pyridylisonicotinamide (3-pina, Scheme 1) or its isomeric dipyridylamide congeners [15–19]. A 3-pina ligand can engage in both supramolecular hydrogen bonding donating and accepting pathways due to its central amide moiety, unlike the kinked dpa or rigid-rod bpy linkers. Different locked conformations are possible for 3-pina ligands when entrained in a coordination polymer network, including *syn* (with the 3-pyridyl ring nitrogen atom positioned on the same side of the molecule as the carbonyl oxygen atom) or *anti* (with the 3-pyridyl ring nitrogen atom positioned on the opposite side of the molecule as the carbonyl oxygen atom, as depicted in Scheme 1). The isostructural phases  $[\text{M}(\text{tere})(3\text{-pina})_2]_n$  ( $\text{M} = \text{Mn}, \text{Co}$ ) display identical (4,4) grid layer

\* Corresponding author.

E-mail address: [laduca@msu.edu](mailto:laduca@msu.edu) (R.L. LaDuca).



Scheme 1. Ligands used in this study.

topologies, with the 3-pina ligands adopting a slightly twisted *syn* conformation in which their 3-pyridyl rings do not ligate [15]. {[Cu(ip)(3-pina)]·H<sub>2</sub>O}<sub>n</sub> (ip = isophthalate) exhibits dimeric units pillared into a non-interpenetrated 3-D 6<sup>5</sup>8 **cds** network by tethering *syn* conformation 3-pina ligands, while {[Cu(tbip)(3-pina)<sub>2</sub>(H<sub>2</sub>O)]·H<sub>2</sub>O}<sub>n</sub> (tbip = 5-*tert*-butylisophthalate) is a 1-D chain coordination polymer with a “butterfly” morphology brought about by *syn* conformation 3-pina ligands whose isonicotinamide 4-pyridyl rings do not ligate [16]. It is thus clear that 3-pina can afford access to a wide variety of coordination polymer topologies in the presence of different aromatic dicarboxylate ligands.

We have therefore attempted to extend this underdeveloped 3-pina coordination chemistry into closed-shell configuration divalent metal systems. In this contribution we report the synthesis, single-crystal structural characterization, luminescent and nitroaromatics sensing properties, and thermal degradation behavior of two new dual-ligand coordination polymers, {[Zn(tere)(3-pina)<sub>2</sub>]·2H<sub>2</sub>O}<sub>n</sub> (**1**) and [Cd(tere)(3-pina)<sub>2</sub>]<sub>n</sub> (**2**). These phases show a very significant change in coordination polymer dimensionality and topology depending on the coordination environment present at the closed shell divalent metal ion.

## 2. Experimental

### 2.1. General considerations

Metal nitrates, terephthalic acid, and nitroaromatics were commercially obtained. Potassium terephthalate was obtained via the reaction of terephthalic acid with excess potassium hydroxide in ethanolic solution. The dipyridylamide ligand 3-pyridylisonicotinamide (3-pina) was prepared by a literature procedure [20]. Water was deionized above 3 M Ω-cm in-house. Elemental analysis was carried out using a Perkin Elmer 2400 Series II CHNS/O Analyzer. IR spectra were recorded on powdered samples using a Perkin Elmer Spectrum One instrument. The luminescence spectra of **1** and **2** were obtained with a Hitachi F-4500 Fluorescence Spectrometer on solid crystalline samples anchored to quartz microscope slides with Rexon Corporation RX-22P ultraviolet-transparent epoxy adhesive. The same Hitachi F-4500 Fluorescence Spectrometer instrument was used for nitroaromatic absorption studies. Thermogravimetric analysis was performed on a TA Instruments Q50 thermal analyzer under flowing N<sub>2</sub>. Topological analysis of coordination polymer networks was carried out using TOPOS software [21].

### 2.2. Preparation of {[Zn(tere)(3-pina)<sub>2</sub>]·2H<sub>2</sub>O}<sub>n</sub> (**1**)

Zn(NO<sub>3</sub>)<sub>2</sub>·6H<sub>2</sub>O (113 mg, 0.38 mmol), 3-pina (74 mg, 0.37 mmol), and potassium terephthalate (89 mg, 0.37 mmol) were mixed with 10 mL of distilled H<sub>2</sub>O in a 23 mL Teflon-lined acid digestion bomb. The bomb was sealed and heated in an oven at 120 °C for 50 h, and then was cooled slowly to 25 °C. Colorless crystals of **1** (95 mg, 77% yield based on 3-pina) were isolated after washing with distilled water, ethanol, and acetone and drying in air. C<sub>30</sub>H<sub>26</sub>N<sub>6</sub>O<sub>8</sub>Zn **1** calc. C, 54.27; H, 3.95; N, 12.66; found C, 54.13; H, 3.91; N, 12.43%. IR ( $\bar{\nu}$ ) = 3064 (w), 1687 (m), 1595 (s), 1556 (s), 1487 (m), 1422 (m), 1393 (m), 1359 (s), 1333 (s), 1303 (s), 1250 (m), 1200 (m), 1131 (w), 1067 (m), 1023 (w), 896 (w), 843 (m), 826 (m), 754 (s), 689 (s), 655 (m) cm<sup>-1</sup>.

**Table 1**  
Crystal and structure refinement data for **1** and **2**.

Data	<b>1</b>	<b>2</b>
Empirical formula	C <sub>30</sub> H <sub>26</sub> N <sub>6</sub> O <sub>8</sub> Zn	C <sub>30</sub> H <sub>22</sub> CdN <sub>6</sub> O <sub>6</sub>
Formula weight	663.94	674.94
Crystal system	monoclinic	monoclinic
Space group	C/2c	P2 <sub>1</sub> /n
<i>a</i> (Å)	21.6696(15)	8.9838(15)
<i>b</i> (Å)	9.2376(5)	7.3016(12)
<i>c</i> (Å)	15.9194(9)	20.264(3)
$\alpha$ (°)	90	90
$\beta$ (°)	115.921(1)	101.657(3)
$\gamma$ (°)	90	90
<i>V</i> (Å <sup>3</sup> )	2866.1(3)	1301.8(4)
<i>Z</i>	4	2
<i>D</i> (g cm <sup>-3</sup> )	1.539	1.722
$\mu$ (mm <sup>-1</sup> )	0.921	0.899
Crystal size (mm)	0.21 × 0.18 × 0.16	0.24 × 0.17 × 0.04
Minimum/maximum trans.	0.9528	0.8447
<i>hkl</i> ranges	−25 ≤ <i>h</i> ≤ 25, −11 ≤ <i>k</i> ≤ 11, −19 ≤ <i>l</i> ≤ 19	−10 ≤ <i>h</i> ≤ 10, −8 ≤ <i>k</i> ≤ 8, −24 ≤ <i>l</i> ≤ 24
Total reflections	22651	10364
Unique reflections	2575	2379
<i>R</i> <sub>int</sub>	0.0303	0.0421
Parameters	212	196
<i>R</i> <sub>1</sub> <sup>a</sup> (all data)	0.0251	0.0342
<i>R</i> <sub>1</sub> <sup>a</sup> ( <i>I</i> > 2σ( <i>I</i> ))	0.0231	0.0260
<i>wR</i> <sub>2</sub> <sup>b</sup> (all data)	0.0585	0.0668
<i>wR</i> <sub>2</sub> <sup>b</sup> ( <i>I</i> > 2σ( <i>I</i> ))	0.0573	0.0621
Maximum/minimum residual (e Å <sup>-3</sup> )	0.333/−0.273	0.393/−0.507
Goodness-of-fit	1.065	1.064

<sup>a</sup>  $R_1 = \sum ||F_o| - |F_c|| / \sum |F_o|$ .

<sup>b</sup>  $wR_2 = \{ \sum [w(F_o^2 - F_c^2)]^2 / \sum [wF_o^2]^2 \}^{1/2}$ .

### 2.3. Preparation of [Cd(tere)(3-pina)<sub>2</sub>]<sub>n</sub> (**2**)

Cd(NO<sub>3</sub>)<sub>2</sub>·4H<sub>2</sub>O (114 mg, 0.37 mmol), 3-pina (74 mg, 0.37 mmol), and potassium terephthalate (89 mg, 0.37 mmol) were mixed with 10 mL of distilled H<sub>2</sub>O in a 23 mL Teflon-lined acid digestion bomb. The bomb was sealed and heated in an oven at 120 °C for 144 h, and then was cooled slowly to 25 °C. Colorless crystals of **2** (112 mg, 89% yield based on 3-pina) were isolated after washing with distilled water, ethanol, and acetone and drying in air. C<sub>30</sub>H<sub>22</sub>CdN<sub>6</sub>O<sub>6</sub> calc. C, 53.39; H, 3.29; N, 12.45; found C, 52.87; H, 3.11; N, 11.98%. IR ( $\bar{\nu}$ ) = 3591 (w), 3056 (w), 2911 (w), 1677 (m), 1560 (s), 1537 (s), 1486 (w), 1424 (m), 1366 (s), 1330 (m), 1303 (s), 1008 (m), 895 (m), 840 (w), 812 (s), 746 (s), 693 (s) cm<sup>-1</sup>.

### 2.4. Nitroaromatic detection studies

A 5 mg sample of coordination polymer **1** or **2** was suspended in 5 mL ethanol in a volumetric flask, with immersion in an ultrasonic bath for 60 s to ensure an even dispersion. The fluorescence spectrum was recorded with an excitation wavelength of 300 nm. Stock solutions of nitrobenzene, *m*-nitrophenol, and benzene (1 × 10<sup>-4</sup> M) in dimethyl sulfoxide were prepared. Aliquots of these stock solutions (10 μL) were added sequentially to coordination polymer ethanol suspensions with sonication for 30 s after each addition. The emission spectra were measured before any analyte addition and after each aliquot of analyte solution.

## 3. X-ray crystallography

Diffraction data for **1** and **2** were collected on a Bruker-AXS SMART-CCD X-ray diffractometer using graphite-monochromated Mo K $\alpha$  radiation ( $\lambda = 0.71073$  Å). The data were processed via SAINT

**Table 2**  
Selected bond distance (Å) and angle (°) data for **1**.

Zn1–O1 <sup>#1</sup>	1.9713(11)	O1–Zn1–N1	103.25(5)
Zn1–O1	1.9713(11)	O1 <sup>#1</sup> –Zn1–N1 <sup>#1</sup>	103.25(5)
Zn1–N1 <sup>#1</sup>	2.0429(13)	O1 <sup>#1</sup> –Zn1–N1	108.78(5)
Zn1–N1	2.0429(13)	O1–Zn1–N1 <sup>#1</sup>	108.78(5)
O1 <sup>#1</sup> –Zn1–O1	108.47(7)	N1–Zn1–N1 <sup>#1</sup>	123.74(8)

Symmetry transformation: #1  $-x + 1, y + 1, -z + 1/2$ .

[22] and subjected to Lorentz effect, polarization effect and absorption corrections using SADABS [23]. The structures were solved using direct methods with SHELXTL [24] using the OLEX2 software suite [25]. All non-hydrogen atoms were refined anisotropically. Hydrogen atoms were placed in calculated positions and refined isotropically with a riding model. Crystallographic details for **1** and **2** are given in Table 1.

## 4. Results and discussion

### 4.1. Synthesis and infrared spectroscopy

Compounds **1** and **2** were prepared cleanly by hydrothermal reaction of the requisite metal nitrate, potassium terephthalate, and 3-pyridylisonicotinamide. Infrared spectra were consistent with the structural components as determined by single-crystal X-ray diffraction. Broad, weak bands at  $\sim 3300\text{ cm}^{-1}$  signify the O–H bonds in the water molecules of crystallization and 3-pina N–H bonds. Weaker, high energy bands at  $\sim 3000\text{--}3200\text{ cm}^{-1}$  are attributed to C–H bond stretching modes in all cases. Asymmetric and symmetric C–O stretching modes of the tere ligands are marked by strong bands at  $1556\text{ cm}^{-1}$  and  $1359\text{ cm}^{-1}$  (**1**) and

**Table 3**  
Selected bond distance (Å) and angle (°) data for **2**.

Cd1–O2 <sup>#1</sup>	2.2168(18)	O2 <sup>#1</sup> –Cd1–N3 <sup>#3</sup>	97.79(7)
Cd1–O2	2.2168(18)	O2–Cd1–N3 <sup>#2</sup>	97.79(7)
Cd1–N1	2.416(2)	O2–Cd1–N3 <sup>#3</sup>	82.21(7)
Cd1–N1 <sup>#1</sup>	2.416(2)	O2 <sup>#1</sup> –Cd1–N3 <sup>#2</sup>	82.21(7)
Cd1–N3 <sup>#2</sup>	2.393(2)	N1–Cd1–N1 <sup>#1</sup>	180.0
Cd1–N3 <sup>#3</sup>	2.393(2)	N3 <sup>#2</sup> –Cd1–N1	85.83(7)
O2 <sup>#1</sup> –Cd1–O2	180.0	N3 <sup>#3</sup> –Cd1–N1 <sup>#1</sup>	85.83(7)
O2–Cd1–N1 <sup>#1</sup>	86.26(7)	N3 <sup>#2</sup> –Cd1–N1 <sup>#1</sup>	94.17(7)
O2–Cd1–N1	93.74(7)	N3 <sup>#3</sup> –Cd1–N1	94.17(7)
O2 <sup>#1</sup> –Cd1–N1 <sup>#1</sup>	93.74(7)	N3 <sup>#3</sup> –Cd1–N3 <sup>#2</sup>	180.00(11)
O2 <sup>#1</sup> –Cd1–N1	86.26(7)		

Symmetry transformations: #1  $-x + 2, -y + 1, -z$ ; #2  $-x + 3/2, -y - 1/2, -z + 1/2$ ; #3  $x + 1/2, -y + 3/2, z - 1/2$ .

$1537\text{ cm}^{-1}$  and  $1366\text{ cm}^{-1}$  (**2**). Sharp, medium intensity bands in the range of  $\sim 1600\text{ cm}^{-1}$  to  $\sim 1200\text{ cm}^{-1}$  are attributed to the stretching modes of the pyridyl rings of the 3-pina ligands [26]. Features corresponding to pyridyl and aryl ring puckering are observed in the region between  $800\text{ cm}^{-1}$  and  $600\text{ cm}^{-1}$ . Sharp, moderate intensity bands at  $1687\text{ cm}^{-1}$  and  $1678\text{ cm}^{-1}$  denote the C=O stretching bands within the amide moieties of the 3-pina ligands for **1** and **2**, respectively.

### 4.2. Structural description of $\{[\text{Zn}(\text{tere})(3\text{-pina})_2]\cdot 2\text{H}_2\text{O}\}_n$ (**1**)

The asymmetric unit of compound **1** contains a divalent zinc atom on a crystallographic 2-fold rotation axis, a complete 3-pina ligand, and half of a tere ligand whose centroid is sited on a crystallographic inversion center, and a water molecule of crystallization. Operation of the rotation axis generates a  $\{\text{ZnO}_2\text{N}_2\}$

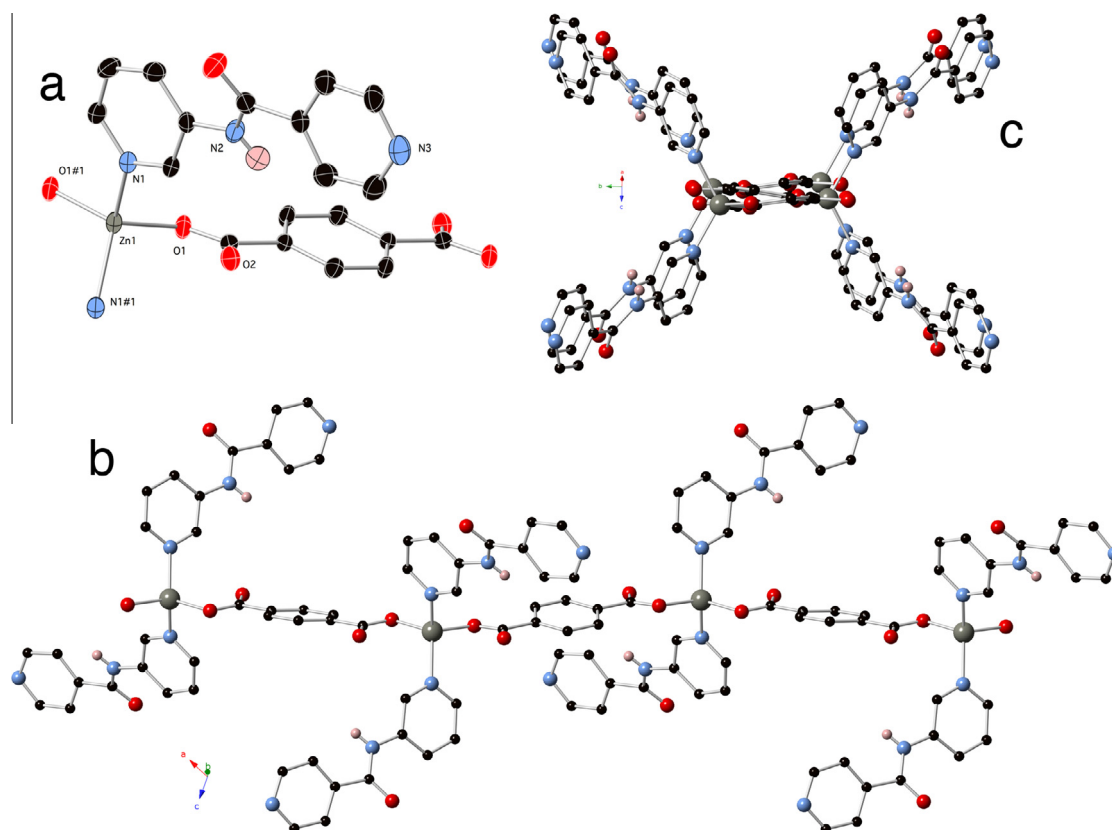


**Fig. 1.** (a)  $\{\text{ZnO}_2\text{N}_2\}$  tetrahedral coordination environment in **1**. Thermal ellipsoids are drawn at 50% probability with symmetry codes as listed in Table 2. (b) Side view of  $[\text{Zn}(\text{tere})(3\text{-pina})_2]_n$  ribbon motif in **1**. (c) View of a single ribbon of **1** down [101].

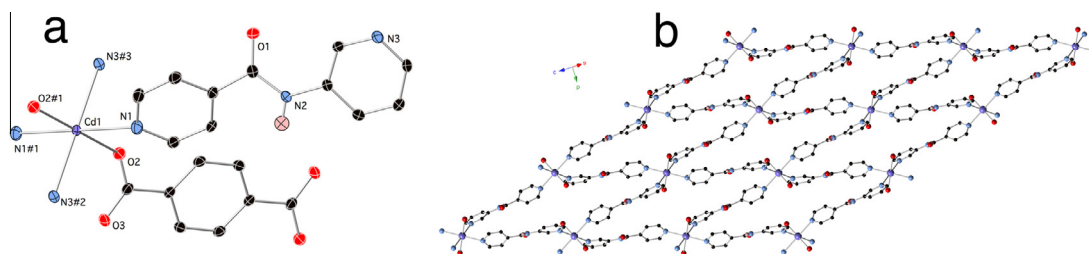


**Fig. 2.** (a)  $\{CdO_4N_2\}$  octahedral coordination environment in **2**. Thermal ellipsoids are drawn at 50% probability. The symmetry codes are listed in Table 3. (b)  $[Cd(3-pina)_2]_n$  (4,4) grid cationic layered motif in **2**.

tetrahedral coordination environment, with the nitrogen donors belonging to the 3-pyridyl rings of two different 3-pina ligands. The isonicotinamide 4-pyridyl nitrogen atoms do not ligate to zinc. The oxygen donors belong to monodentate carboxylate groups of two different tere ligands. Bond lengths and angles within the tetrahedral coordination environment are listed in Table 2, with a thermal ellipsoid plot depicted in Fig. 1a.

Bis(monodentate) tere ligands conjoin divalent zinc atoms into neutral zig-zag  $[Zn(tere)]_n$  chain motifs with a  $Zn \cdots Zn$  distance of 11.098 Å. These are decorated by the monodentate *anti* conformation 3-pina ligands to afford neutral  $[Zn(tere)(3-pina)_2]_n$  ribbons (Fig. 1b). Viewing the ribbon motif down  $[101]$  gives a perspective of an “X” shape (Fig. 1c). Adjacent  $[Zn(tere)(3-pina)_2]_n$  ribbons aggregate (Fig. S1) by hydrogen bonding patterns (Table S1) involving isolated water molecules of crystallization located in small solvent-accessible pockets comprising 2.0% of the unit cell volume according to PLATON [27]. The water molecules of crystallization accept hydrogen bonds from N–H groups within the amide functional groups of the 3-pina ligands, and donate hydrogen bonds to unligated isonicotinamide pyridyl nitrogen atoms in 3-pina

ligands and to unligated tere carboxylate oxygen atoms in neighboring ribbons. Non-classical C–H $\cdots$ O hydrogen bonding interactions between tere aromatic carbon atoms, and the carbonyl group within 3-pina ligands in neighboring ribbons, serve an ancillary role in the inter-ribbon aggregation.

#### 4.3. Structural description of $[Cd(tere)(3-pina)_2]_n$ (**2**)

The asymmetric unit of compound **2** contains a divalent cadmium atom on a crystallographic inversion center, half of a tere ligand whose centroid rests on another inversion center, and a complete 3-pina ligand. Operation of the crystallographic inversion center generates a  $\{CdO_2N_4\}$  distorted octahedral coordination environment, with trans nitrogen donor atoms belonging to the 3-pyridyl rings of two different 3-pina ligands, and another set of trans nitrogen donor atoms belonging to the isonicotinamide pyridyl rings of two additional 3-pina ligands. The oxygen atom donors are provided by two tere ligands. Bond lengths and angles within the octahedral coordination environment at cadmium are listed in Table 3, and a thermal ellipsoid plot is drawn in Fig. 2a.

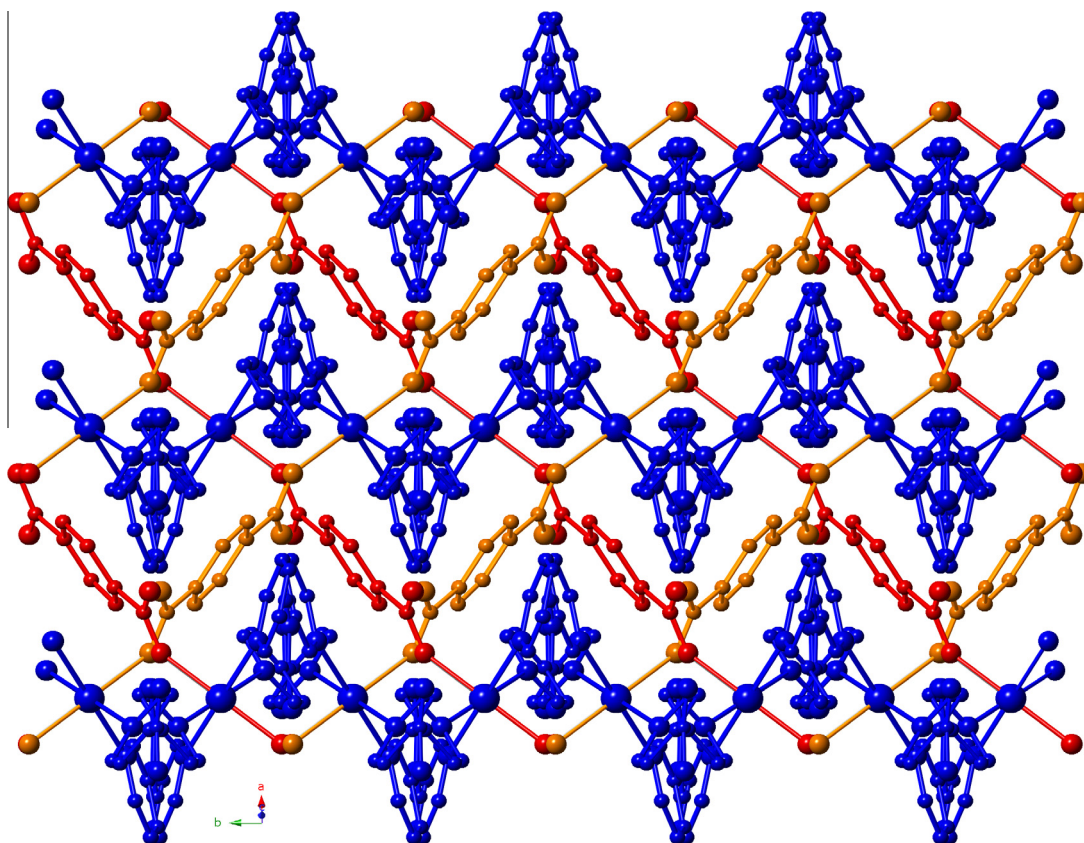


**Fig. 3.**  $[Cd(tere)(3-pina)_2]_n$  3-D self-penetrated coordination polymer network in **2**.

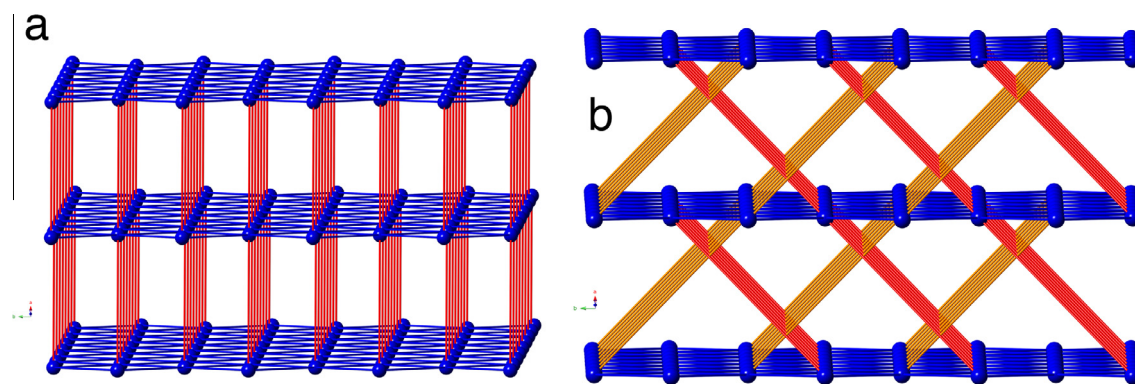


**Fig. 4.** (a) Schematic perspective of a traditional straight-pillared  $pcu$   $4^{12}6^3$  topology. (b) Schematic perspective of the  $4^{46}108$   $mab$  topology cross-pillared 3-D self-penetrated net in **2**.

Cadmium atoms are connected into cationic  $[Cd(3-pina)_2]_n$  (4,4) coordination polymer grid motifs (Fig. 2b) by tethering *syn* conformation 3-pina ligands, that span a Cd...Cd distance of 12.432 Å. The grid apertures are rather pinched, with through-space Cd...Cd distances of 7.302 and 23.768 Å; the Cd...Cd...Cd angles around the perimeter of all the grid windows measure 34.1° and 145.9°. The cationic  $[Cd(3-pina)_2]_n$  layers in **2** are situated parallel to the (101) crystal planes.

Parallel  $[Cd(3-pina)_2]_n$  layers stack along (100), with a closest Cd...Cd contact distance of 8.984 Å that matches the *a* lattice parameter. However, this distance is too small to be pillared by any charge-balancing tere ligands. Instead the bis(monodentate) tere ligands connect cadmium atoms in neighboring layers in a crossed fashion in order to span a Cd...Cd distance of 11.577 Å in the resulting  $[Cd(tere)(3-pina)_2]_n$  3-D coordination polymer network (Fig. 3). Straight pillaring would result in a standard  $4^{12}6^3$   $pcu$  primitive-cubic like network (Fig. 4a), but the crossed pillaring necessitated by the long span of the tere ligands in **2** affords a 6-connected  $4^{46}108$   $mab$  self-penetrated network (Fig. 4b). There

have been some previous reports of this self-penetrated  $mab$  topology [28–30]. However, most of these prior phases feature metal dicarboxylate layers with paddlewheel dinuclear units pillared by dipyriddy ligands, for example in  $[Cu_2(glutarate)_2(bpmp)]_n$  (*bpmp* = bis(4-pyridylmethyl)piperazine) [28]. Compound **2** thus represents a rare example of a metal-dipyridyl layered coordination polymer pillared into a self-penetrated network by the dicarboxylate ligands. There are no solvent-accessible voids within the self-penetrated network of **2**.

#### 4.4. Thermal properties

Compound **1** underwent dehydration between 85 and 110 °C, with a mass loss of 5.8% corresponding well with the predicted value for two molar equivalents of water (5.4%). Combustion of the organic ligands occurred above 240 °C. The mass of compound **2** remained stable until 330 °C, whereupon ligand ejection occurred. TGA traces for **1** and **2** are shown in Figs. S2 and S3.

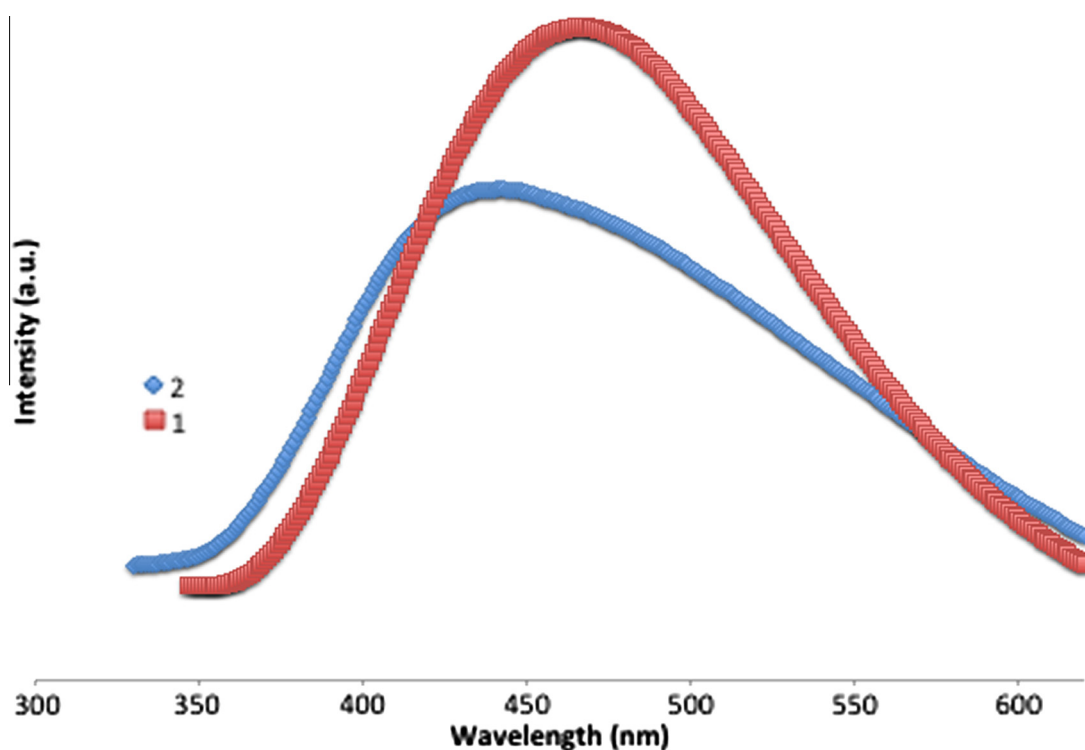


**Fig. 5.** Solid-state emission spectra of **1** and **2**.

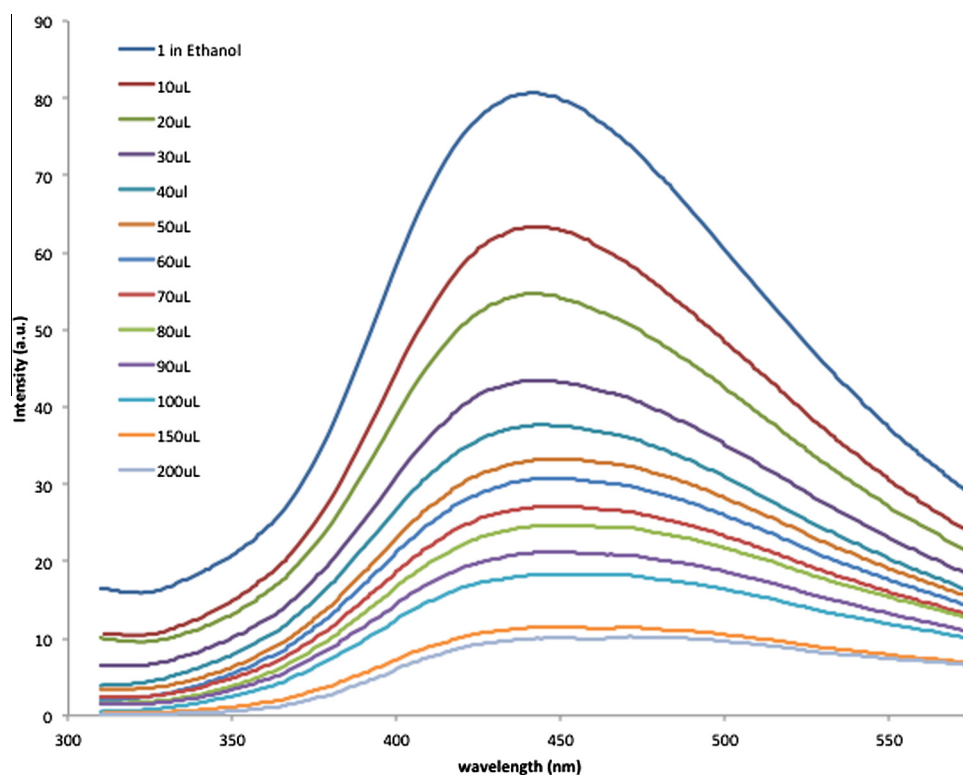


Fig. 6. Emission profiles of **1** in ethanol suspension, in the presence of varying amounts of a  $1 \times 10^{-4}$  M DMSO solution of nitrobenzene.

#### 4.5. Luminescence spectra

Solid samples of **1** and **2** were irradiated with ultraviolet light to examine their photoluminescent behavior. The excitation spectra for **1** and **2** were recorded by monitoring emission at 400 nm,

revealing maximum excitation wavelengths of 337 nm and 320 nm, respectively. Upon excitation at this wavelength, modest blue-violet visible light emission was observed in both cases. The emission maxima for **1** and **2** were 467 nm and 441 nm, respectively (Fig. 5). When the pure 3-pina ligand was irradiated at

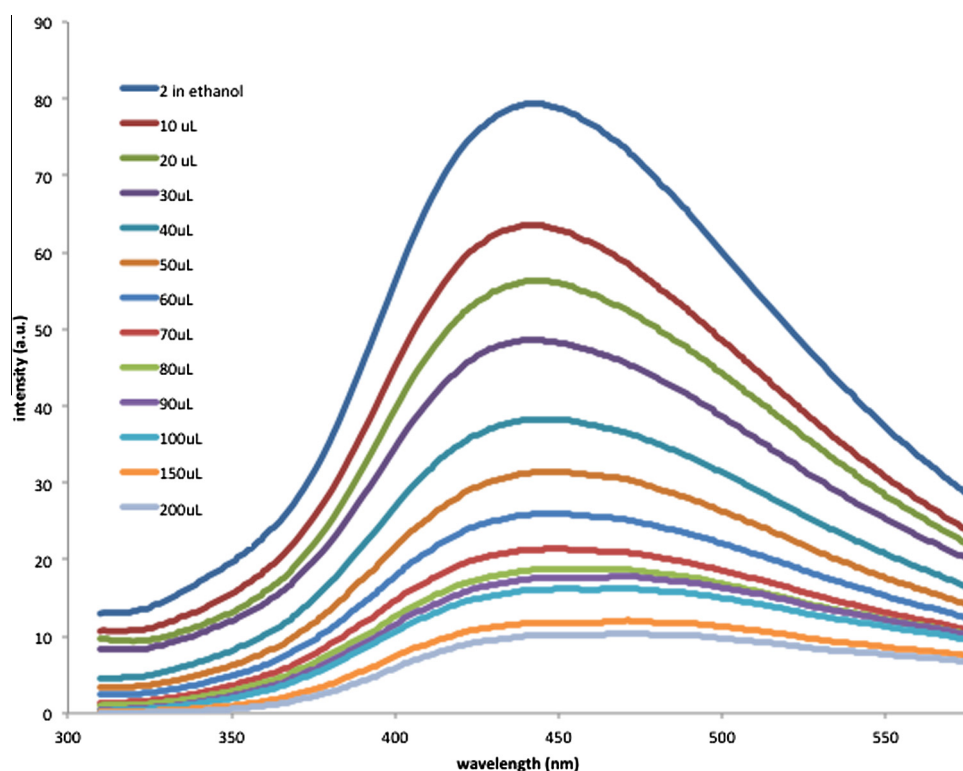


Fig. 7. Emission profiles of **2** in ethanol suspension, in the presence of varying amounts of a  $1 \times 10^{-4}$  M DMSO solution of nitrobenzene.

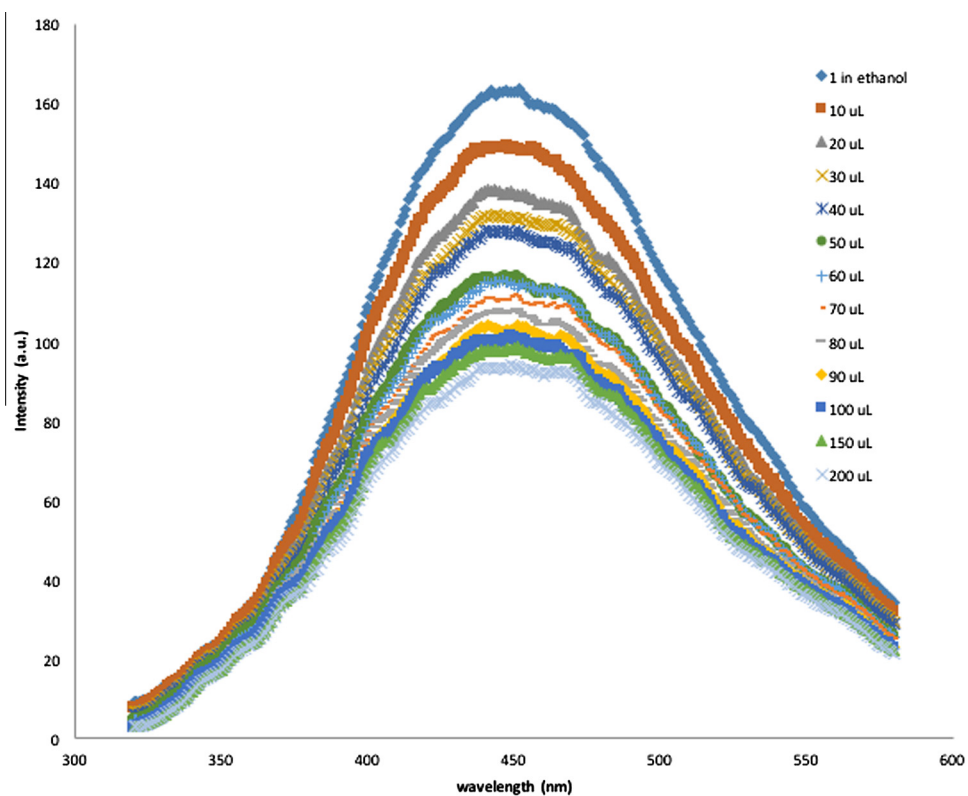


Fig. 8. Emission profiles of 1 in ethanol suspension, in the presence of varying amounts of a  $1 \times 10^{-4}$  M DMSO solution of *m*-nitrophenol.

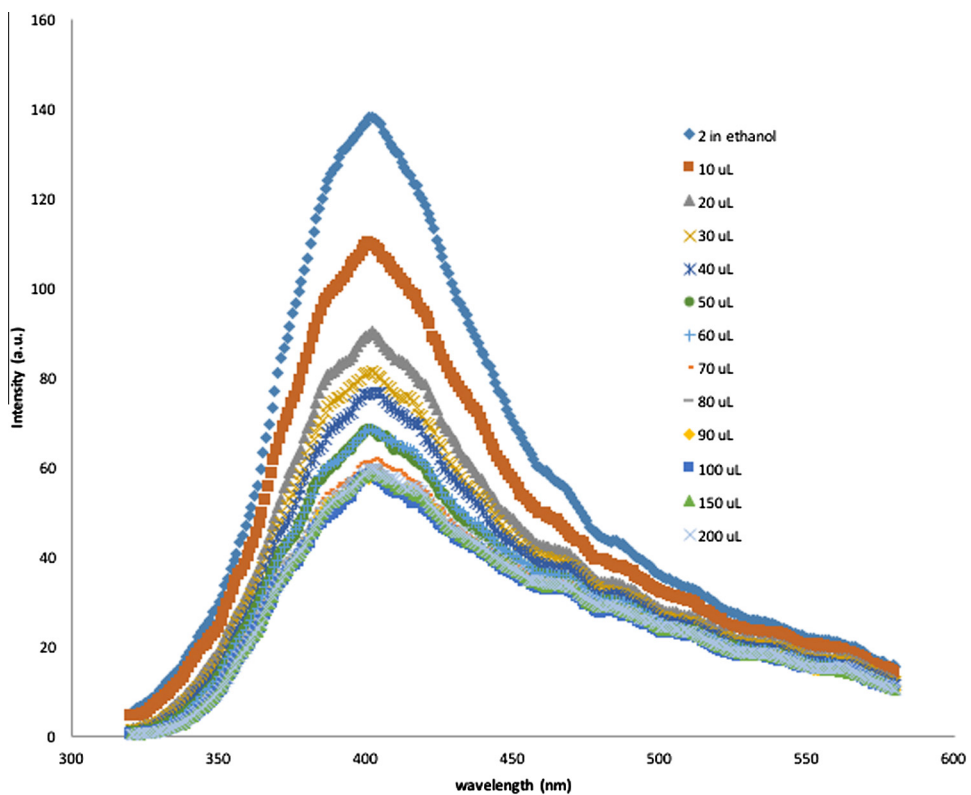


Fig. 9. Emission profiles of 2 in ethanol suspension, in the presence of varying amounts of a  $1 \times 10^{-4}$  M DMSO solution of *m*-nitrophenol.

265 nm, a blue emission with broad spectral profile centered at 465 nm was observed (Fig. S4). The fluorescent properties of **1** and **2** are ascribed to  $\pi$ - $\pi^*$  molecular orbital transitions within the aromatic ring systems of the 3-pina and tere ligands [7].

#### 4.6. Nitroaromatic sensing

Both compounds **1** and **2** show capability for detection of nitrobenzene (Figs. 6 and 7, respectively) and *m*-nitrophenol (Figs. 8 and 9, respectively) in ethanol suspension. Addition of small aliquots of nitroaromatic compounds dissolved in DMSO ( $1 \times 10^{-4}$  M) resulted in diminution of the coordination polymer luminescence intensity upon excitation with ultraviolet light ( $\lambda_{\text{ex}} = 300$  nm). This loss of emission signal is attributed to charge transfer from the excited states of the ligand molecular orbitals within the coordination polymer, to those of the adsorbed electron-withdrawing nitroaromatic substrate [5]. As control experiments, aliquots of a benzene solutions in DMSO ( $1 \times 10^{-4}$  M) were added to ethanol suspensions of both **1** and **2**. Only a very small decrease in luminescence intensity was observed in either case (Figs. S5 and S6, respectively). Thus, it is averred that coordination polymers **1** and **2** are functional detectors for nitroaromatic compounds. Both compounds **1** and **2** show enhanced absorption of nitrobenzene compared to the more sterically bulky *m*-nitrophenol. For nitrobenzene, the intensity factor  $(I_0 - I)/I_0$  ( $I_0 =$  maximum intensity in the absence of analyte) reaches a level about 13% of the initial  $I_0$  value for both **1** and **2** after 200  $\mu\text{L}$  of the stock analyte solution was added (Figs. S7 and S8). For *m*-nitrophenol, the comparable intensity factor reaches 0.57 and 0.43 for **1** and **2**, respectively. The 3-D structure of compound **2** thus appears to be able to absorb more *m*-nitrophenol than the 1-D structure of compound **1** (Figs. S9 and S10).

## 5. Conclusions

A pair of closed-shell divalent metal terephthalate coordination polymers with ancillary 3-pina ligands has been prepared and structurally characterized. Although both the zinc and cadmium derivatives have the same ratio of ligands and a similar bis(monodentate)terephthalate binding mode, their structural topologies are radically different. The smaller ionic radius of zinc affords a 4-coordinate tetrahedral arrangement of donors. As the pendant 4-pyridyl donor atoms of the 3-pina ligands cannot bind, a zig-zag chain motif is observed in **1**. Expansion of the coordination sphere to octahedral, due to the larger ionic radius of cadmium, results in the ability to ligate all of the 3-pina donor atoms, which instills the generation of the 3-D net seen in **2**. As the interlayer spacing is too small for direct terephthalate bridging, an uncommon 6-connected self-penetrated network is observed in the cadmium derivative. Ancillary structure-directing effects provided by different 3-pina conformations (*anti* in **1**, *syn* in **2**) and amide group hydrogen bonding patterns act in a synergistic fashion with the predominating coordination environment effects. The self-penetration of the coordination polymer network in **2** resulted in added thermal stability. Both materials show promise as sensors for the detection of nitroaromatic compounds in solution, with a preference for less sterically bulky analytes.

## Acknowledgements

Funding for the work was provided by Lyman Briggs College of Michigan State University. We thank Dr. Rui Huang for elemental analysis.

## Appendix A. Supplementary data

CCDC 1048725 and 1048726 contains the supplementary crystallographic data for **1** and **2**. These data can be obtained free of charge via <http://www.ccdc.cam.ac.uk/conts/retrieving.html>, or from the Cambridge Crystallographic Data Centre, 12 Union Road, Cambridge CB2 1EZ, UK; fax: (+44) 1223-336-033; or e-mail: [deposit@ccdc.cam.ac.uk](mailto:deposit@ccdc.cam.ac.uk). Supplementary data associated with this article can be found, in the online version, at <http://dx.doi.org/10.1016/j.poly.2015.10.011>.

## References

- (a) M.P. Suh, H.J. Park, T.K. Prasad, D. Lim, *Chem. Rev.* **112** (2012) 782; (b) L.J. Murray, M. Dinca, J.R. Long, *Chem. Soc. Rev.* **38** (2009) 1294. and references therein.
- (a) K. Sumida, D.L. Rogow, J.A. Mason, T.M. McDonald, E.D. Bloch, Z.R. Herm, T. Bae, J.R. Long, *Chem. Rev.* **112** (2012) 724; (b) J.R. Li, R.J. Kuppler, H.C. Zhou, *Chem. Soc. Rev.* **38** (2009) 1477. and references therein; (c) J. Li, J. Sculley, H. Zhou, *Chem. Rev.* **112** (2012) 869.
- L. Bastin, P.S. Barcia, E.J. Hurtado, J.A.C. Silva, A.E. Rodrigues, B. Chen, *J. Phys. Chem. C* **112** (2008) 1575.
- (a) J. Liu, L. Chen, H. Cui, J. Zhang, L. Zhang, C. Su, *Chem. Soc. Rev.* **43** (2014) 6011. and references therein; (b) J. Lee, O.K. Farha, J. Roberts, K.A. Scheidt, S.T. Nguyen, J.T. Hupp, *Chem. Soc. Rev.* **38** (2009) 1450. and references therein; (c) L. Ma, C. Abney, W. Lin, *Chem. Soc. Rev.* **38** (2009) 1248. and references therein.
- (a) Z. Hu, B.J. Deibert, J. Li, *Chem. Soc. Rev.* **43** (2014) 5815; (b) G. Wang, L. Yang, Y. Li, H. Song, W. Ruan, Z. Chang, X. Bu, *Dalton Trans.* **42** (2013) 12865.
- L. Carlucci, G. Ciani, D.M. Proserpio, *Coord. Chem. Rev.* **246** (2003) 247. and references therein.
- M.D. Allendorf, C.A. Bauer, R.K. Bhakta, R.T. Houk, *Chem. Soc. Rev.* **38** (2009) 1330. and references therein.
- C. Wang, T. Zhang, W. Lin, *Chem. Rev.* **112** (2012) 1084. and references therein.
- P. Lightfoot, A.J. Snedden, *J. Chem. Soc., Dalton Trans.* (1999) 3549.
- E. Shyu, R.M. Supkowski, R.L. LaDuca, *Inorg. Chem.* **48** (2009) 2723.
- B. Chen, C. Liang, J. Yang, D.S. Contreras, Y.L. Clancy, E.B. Lobkovsky, O.M. Yaghi, S. Dai, *Angew. Chem., Int. Ed.* **45** (2006) 1390.
- J.Y. Baeg, S.W. Lee, *Inorg. Chem. Commun.* **6** (2003) 313.
- J. Tao, X.M. Chen, R.B. Huang, L.S. Zheng, *J. Solid State Chem.* **170** (2003) 130.
- H.J. Park, M.P. Suh, *Chem. Commun.* (2010) 610.
- J.S. Goldsworthy, A.L. Pochodylo, R.L. LaDuca, *Inorg. Chim. Acta* **419** (2014) 26.
- M.E. O'Donovan, A.R. Porta, M.D. Torres Salgado, R.L. LaDuca, *Z. Anorg. Allg. Chem.* **640** (2014) 2113.
- J.A. Wilson, J.W. Uebler, R.L. LaDuca, *CrystEngComm* **15** (2013) 5218.
- N.H. Murray, R.L. LaDuca, *Inorg. Chim. Acta* **421** (2014) 145.
- A.L. Pochodylo, J.A. Wilson, J.W. Uebler, S.H. Qiblawi, R.L. LaDuca, *Inorg. Chim. Acta* **423** (2014) 298.
- T.S. Gardner, E. Wenis, J.J. Lee, *J. Org. Chem.* **19** (1954) 753.
- V.A. Blatov, A.P. Shevchenko, D.M. Proserpio, *Cryst. Growth Des.* **14** (2014) 3576. TOPOS software is available for download at: <http://www.topospro.com>.
- SAINT, Software for Data Extraction and Reduction, Version 6.02, Bruker AXS Inc, Madison, WI, 2002.
- SADABS, Software for Empirical Absorption Correction, Version 2.03, Bruker AXS Inc, Madison, WI, 2002.
- G.M. Sheldrick, *Acta Crystallogr. A* **64** (2008) 112.
- O.V. Dolomanov, L.J. Bourhis, R.J. Gildea, J.A.K. Howard, H. Puschmann, *J. Appl. Crystallogr.* **42** (2009) 229.
- M. Kurmoo, C. Estourmes, Y. Oka, H. Kumagai, K. Inoue, *Inorg. Chem.* **44** (2005) 217.
- A.L. Spek, PLATON, A Multipurpose Crystallographic Tool, Utrecht University, Utrecht, The Netherlands, 1998.
- D.P. Martin, R.M. Supkowski, R.L. LaDuca, *Cryst. Growth Des.* **10** (2008) 3518.
- M.A. Braverman, R.L. LaDuca, *CrystEngComm* **10** (2008) 117.
- J.W. Uebler, A.L. Pochodylo, R.J. Staples, R.L. LaDuca, *Cryst. Growth Des.* **13** (2013) 2220.